Up-down separation and debubble using a multicomponent non-stationary prediction-error filter

Kaiwen Wang, Joseph Jennings and Jon Claerbout, Stanford University*

SUMMARY

Marine data recorded on ocean-bottom nodes (OBN) benefit greatly from bubble removal and wavefield decomposition. The prediction-error filter (PEF) method is known to work well on single channel bubble removal. In this study, we extend the single component PEF to apply it on multicomponent recordings for both bubble removal and wavefield separation. We test our method on a synthetic example and then apply it on real data. The results show that our method performs well in bubble removal and wavefield separation for upgoing and downgoing components. Our method does not rely on the stationary statistics assumption and requires little prior knowledge of the physical model.

INTRODUCTION

Marine seismic data with active source provides us a valuable opportunity to image structures below the seafloor. However, the data recorded by ocean-bottom nodes (OBN) are often contaminated by airgun bubbles and ocean bottom reflections following the main arrival. Removing the effect of the bubble and separating the upgoing and downgoing waves would largely help improve the imaging quality.

Several methods has been developed to solve the debubble and up-down separation problem. Claerbout *et al.*(2019) proposed non-stationary PEF in order to debubble single component data. Melbø *et al.*(2002) designed a hydrophone and vertical component (PZ) calibration approach by minimizing the energy in a manually picked refracted wave window. In this study, we extend the non-stationary PEF method by Claerbout *et al.*(2019) in order to apply it on multicomponent data. Instead of assuming stationary data statistics to calculate a calibration filter based on a certain preselected rule, we allow the data statistics to vary with time and space. As we feed in data, our multicomponent PEF updates based on new data statistics. Therefore, our method has the advantage that it requires little human intervention and prior knowledge of the physical model parameters.

THEORY

We extend the non-stationary PEF deconvolution by Claerbout *et al.*(2019) into vector signals. The two-component PEF structure designed for separating upgoing and downgoing wavefield is shown in Figure 1. Our theory contains two parts which act as non-stationary systems: the PEF and wavefield separation. The two systems are updated jointly at each time step to learn non-stationary statistics.

Non-stationary PEF

The stationary PEF or auto-regression technique has been well developed in the twentieth century. Claerbout *et al.*(2019) broke the assumption of stationarity and formulated the non-stationary realization which allowed the PEF to vary with time and space. Here we follow their parameter update rule for the PEF shown in Figure 2. At time t, a filter of certain length is convolved with the data underneath it to predict the next data point. The prediction error is back-projected to give gradients for filter update. At the next time step $t+1$, we go over the same forward prediction and parameters update step. The process is repeated until we pass through all the data in time and space. To remove the bubble signature, we choose a lagged PEF which forces the end portion of the filter to be all zeros. We set the length of lag to be comparable to the bubble interval so that the bubble can be predicted by the initial source response.

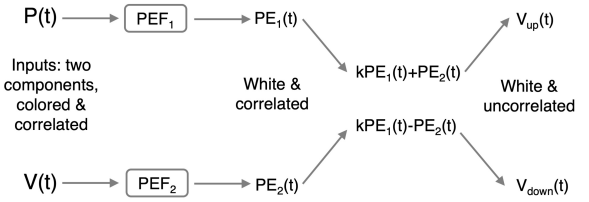

Figure 1: Multicomponent non-stationary PEF structure. P and V are pressure and vertical velocity recorded at the same node. PEF is prediction error filter at time step t. PE is prediction error of time t. k is a scaling factor. V_{up} and V_{down} are separated upgoing and downgoing velocity wavefield.

Figure 2: Illustration of non-stationary one-component PEF update.

Non-stationary wavefield separation

The acoustic decomposition of ocean bottom node data requires a set of parameter inputs: water density, vertical slowness and calibration filter. Here we follow a similar workflow where calibrated pressure component and vertical component can be decorrelated (Figure 3). The inputs (on the left of the equations in Figure 3) consist of prediction errors of pressure and vertical components. The pressure prediction errors are scaled by factor k to convert to correct units (particle velocity) and to project the oblique incoming waves to vertical direction. The vertical component prediction errors are then added to or subtracted from the scaled pressure component prediction errors to cancel the cross-talk. Our method is different from the

10.1190/segam2019-3215841.1

original acoustic decomposition in that we do not need prior knowledge of those physical parameters. Instead, we learn the non-stationary scaling factor k as we pass through the data. The scaling factor k is updated at each time step to minimize cross-talk energy. In this way, we make it a data-driven process for designature and wavefield separation.

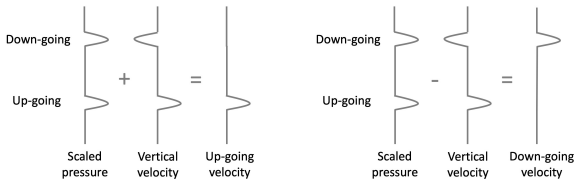

Figure 3: Acoustic decomposition of prediction errors.

EXAMPLE

We first test our method on a simple synthetic test. We then apply the multicomponent non-stationary PEF on a real dataset of ocean bottom nodes. The results are shown in the following subsections.

Synthetic test

To test our method, we set up a simple synthetic model shown in Figure 4. We mimic the ocean bottom survey geometry by a single source on the top and a receiver line on the bottom. The model has homogeneous velocity and free surface on the top and bottom boundary. We generate two component (pressure and vertical velocity component) recordings using finite difference modeling of the acoustic wave equation.

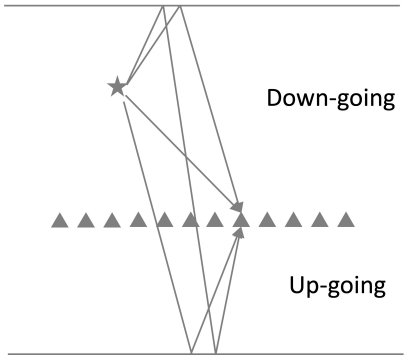

Figure 4: Model for synthetic test.

The synthetic hydrophone and vertical recordings are shown in Figure 5. We see from the plot that the upgoing and downgoing waves alternate in the recordings. The first two arrivals are downgoing waves, which have same polarity in the hydrophone and vertical components. The two ray-paths are plotted in Figure 4. The next two arrivals are both upgoing waves, which have reverse polarity in the hydrophone and vertical components. The two corresponding upgoing ray-paths are also plotted in Figure 4.

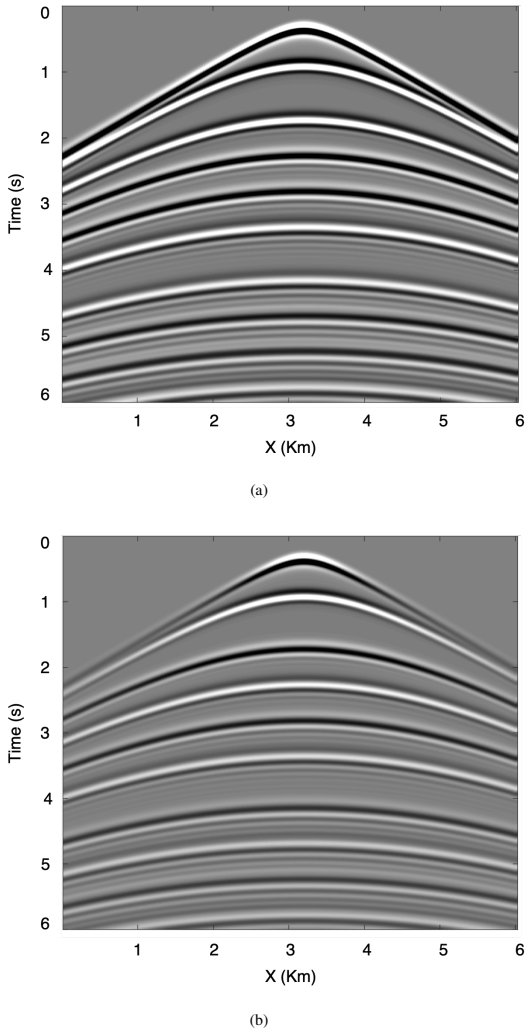

Figure 5: Synthetic shot gathers generated via finite difference modeling. Panel (a) shows the hydrophone data and (b) the vertical velocity data.

We applied our multicomponent PEF to separate and deconvolve the upgoing and downgoing wavefield. The separation and deconvolution results are shown in Figure 6. We see from the separation results that the upgoing and downgoing wavefields are separated successfully except for some artifacts. One of sources of the artifacts source is the numerical dispersion from the finite difference simulation. Those high frequency dispersion tails cannot be predicted so they remain in the prediction errors. The artifacts at the beginning of each trace (about 100 samples long) come from the way we pass though the data. We set the PEF at the end of each trace to be the initial value of the beginning of the next trace. The length of this artifact suggests that our non-stationary filter takes about 100 time steps to learn new data statistics. Figure 7 shows the changes in our non-stationary scaling factor k. We know from its physical meaning that k should be proportional to $\cos\theta$, where θ is

10.1190/segam2019-3215841.1

the incidence angle. We confirmed that behavior in Figure 7. From our model setup (Figure 4), k at trace 100 should have $\theta = 0$. When we go to further offset, the θ increases and $\cos\theta$ decreases, so we can see decreasing k at further offset.

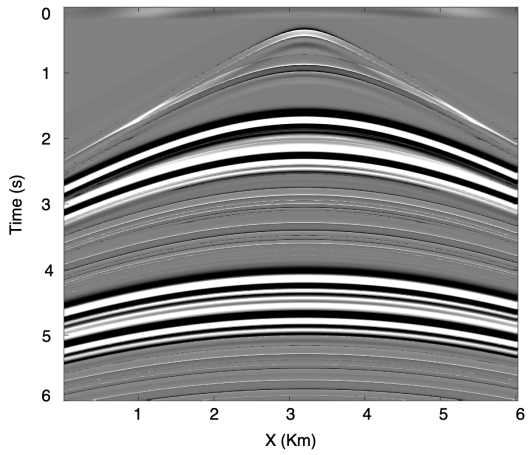

(a)

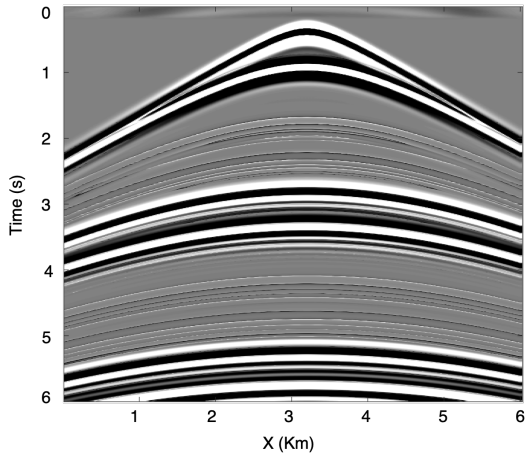

(b)

Figure 6: Results of deconvolution and wavefield separation of synthetic hydrophone and vertical particle velcoty data shown in Figure 5. Panel (a) shows the separated upgoing wavefield and (b) shows the separated downgoing wavefield.

Real data

After we tested our method on a simple synthetic model, we next applied it on a real dataset. The dataset is a 3D GOM OBN dataset. We show here an example of a receiver gather recorded from a line of shots traversing across the node. We first corrected for the instrument response of each of the two components. The data after instrument response correction are shown in Figure 8. Two components (hydrophone and vertical) are used in this example. Each has 200 shots and was windowed to six seconds of recording length. We see that both components in Figure 8 have strong bubbles and the vertical geophone component has shear noise. The upgoing and downgoing waves are also mixed and hidden under the bubbles.

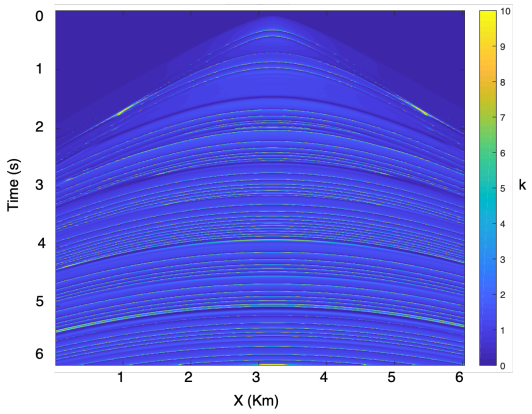

Figure 7: The estimated non-stationary scaling factor k displayed as a function of space and time.

We applied a multicomponent non-stationary PEF on the hydrophone and vertical components to output debubbled and separated upgoing and downgoing velocity wavefields. We use a 100-sample long filter with a 60 sample lag. The initial values of PEF coefficients are set to be a vector of small uniformly-distributed random numbers. The initial value of scaling factor k is one. The learning rate for PEF update is 20. We show the results of debuble and wavefield separation in Figure 9. From Figure 9 we see that the bubbles are effectively removed, revealing complex, higher-frequency features of the wavefields. The effect of the bubble on the upgoing component (Figure 9a) is almost invisible. This suggests that our PEF is learning the bubble statistics well and can adapt as the bubble signature changes. The bubbles on the downgoing component are also clearly reduced. However, we can still observe some high frequency weak bubbles after the direct arrival. This suggests that we might need a PEF with shorter a lag on one of the components. The up-down separation step also functions well in the real data case. Comparing Figure 9a and b, we can see that the critically refracted waves are mainly on the upgoing component while the multiple reflections of the direct arrival fall into the downgoing component.

CONCLUSION

In this study, we extended the single component non-stationary PEF to vector recordings and designed a multicomponent non-stationary PEF to jointly debubble and separate the wavefields into different causes. We tested our method on a synthetic example and demonstrated it on a real dataset. We show that our method performs well without knowing any prior information of the physical parameters or the source wavelet. Our model update is data driven and fully automatic. One distinct advantage of our method is that we do not make stationary assumption so that the filter can learn from data with changing statistics.

10.1190/segam2019-3215841.1

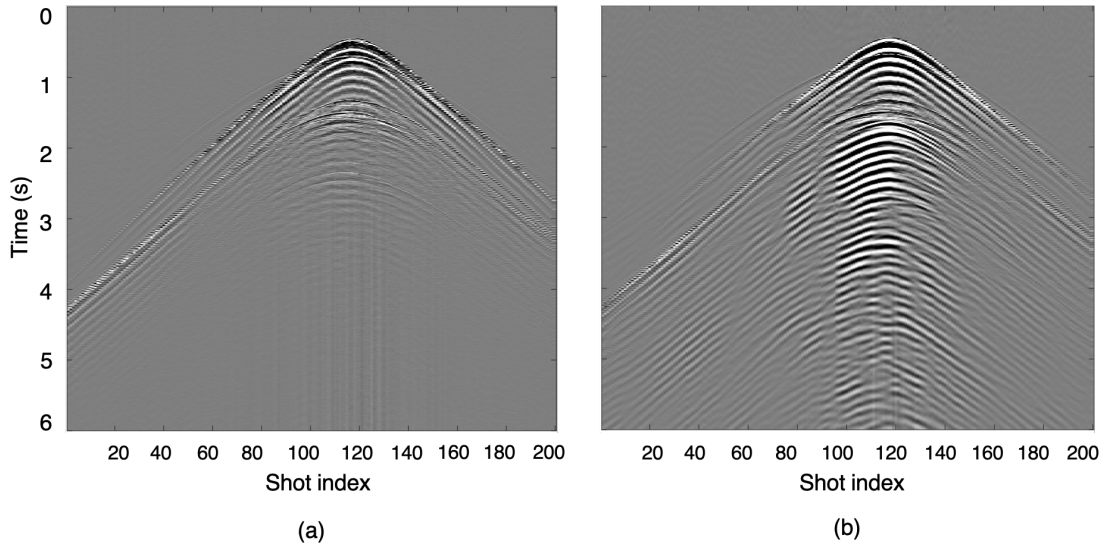

Figure 8: Data from OBN receiver gather that served as input to our wavefield separation and debubble algorithm. (a) Hydrophone component. (b) Vertical particle velocity component.

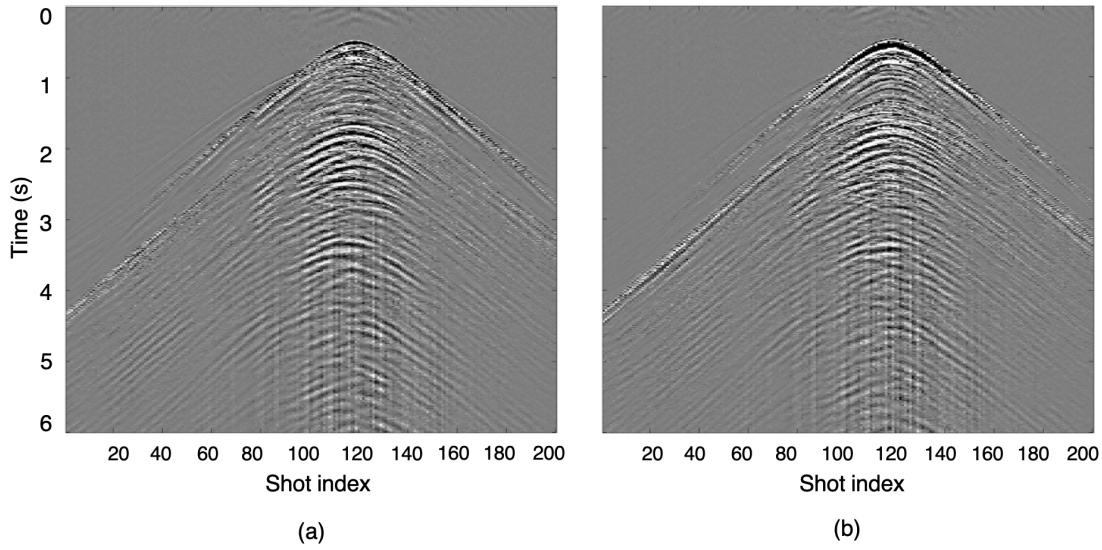

Figure 9: Results of joint debubble and wavefield separation applied to the data shown in Figure 8. Panel (a) shows the separated upgoing wavefield and panel (b) shows the downgoing wavefield.

ACKNOWLEDGMENTS

We would like to thank Shell Exploration and Production Company for the 3D GOM OBN dataset used in this study. We thank Taylor Dahlke for removing instrument response from the raw data.

REFERENCES

Claerbout, J. F., A. Guitton, S. A. Levin, and K. Wang, 2019, Data fitting with nonstationary statistics: https://doi.org/Lulu.com.
Melbø, A. H., J. O., Robertsson, and D.-J., van Manen, 2002, PZ calibration by applying the equation of motion to critically refracted waves: 72nd Annual International Meeting, SEG, Expanded Abstracts, 1030–1033, doi: https://doi.org/10.1190/1.1816819.